Applied Catalysis B: Environmental 113–114 (2012) 87–99

Contents lists available at SciVerse ScienceDirect

Applied Catalysis B: Environmental

journal homepage: www.elsevier.com/locate/apcatb

Simultaneous hydrodesulfurization and hydrodenitrogenation on MoP/SiO_2 catalysts: Effect of catalyst preparation method

A. Infantes-Molina[a,**], C. Moreno-León[b], B. Pawelec[a], J.L.G. Fierro[a], E. Rodríguez-Castellón[b], A. Jiménez-López[b,*]

[a] Instituto de Catálisis y Petroleoquímica, CSIC, Cantoblanco, 28049 Madrid, Spain
[b] Departamento de Química Inorgánica, Cristalografía y Mineralogía (Unidad Asociada al ICP-CSIC), Facultad de Ciencias, Universidad de Málaga, Campus de Teatinos, 29071 Málaga, Spain

ARTICLE INFO

Article history:
Received 2 August 2011
Received in revised form
14 November 2011
Accepted 16 November 2011
Available online 23 November 2011

Keywords:
Silica
Molybdenum phosphide
Dibenzothiophene
HDS
Quinoline
HDN

ABSTRACT

Silica-supported MoP catalysts were prepared by temperature-programmed reduction (H_2-TPR) at 550, 600 and 700 °C of the corresponding dried or calcined substrates. Two catalysts were prepared by using two different synthetic approaches. A MoP catalyst was prepared using the method described in the literature that uses ammonium phosphate ($NH_4H_2PO_4$) and ammonium heptamolybdate ($(NH_4)_6Mo_7O_{24}{\cdot}4H_2O$) precursors, calcination and subsequent H_2-TPR at high temperature. A new synthetic approach was carried out to prepare another MoP catalyst using ammonium molybdate ($(NH_4)_2MoO_4$) and phosphorous acid (H_2PO_3H) as precursors and subsequent H_2-TPR. The catalytic activity was evaluated in the individual and simultaneous hydrodesulfurization (HDS) and hydrodenitrogenation (HDN) reactions performed in a flow reactor under a hydrogen pressure of 3.0 MPa. The fresh reduced and spent catalysts were characterized by ICP, N_2 adsorption–desorption isotherms at −196 °C, XRD, HRTEM, NH_3-TPD, XPS and elemental chemical CNHS analysis. The silica-supported MoP catalysts prepared by the new synthetic method were more active in the HDS of DBT than the catalyst prepared by reduction of calcined substrate. The catalyst characterization results showed that the lower reduction temperature required to form the MoP species is responsible for the enhancement in catalytic performance. The key factors influencing on the catalytic activity are: a large specific surface area, high acidity and good dispersion of MoP phase on the support substrate. Activity measurements in simultaneous HDN–HDS showed that quinoline conversion is enhanced in the presence of a small amount of DBT whereas the HDS of DBT reaction does not appear to be inhibited by a small amount of quinoline added to the feed.

1. Introduction

In order to achieve a large reduction of S- and N-content in fuels due to more stringent environmental restrictions and lower quality of the remnant petroleum reserves, improved methods for removal of organosulfur and organonitrogen compounds from fuel will become of greater importance. Therefore, new catalytic phases highly active for hydrotreating reactions are being claimed. Actually more efficient catalytic systems are being searched combining Ni, Mo, W and Co transition metals with carbon [1,2], nitrogen [1,3] and recently phosphorus [4,5], becoming a promising alternative to the traditional sulfides. Nitrides and carbides are unstable under the presence of H_2S as long as they are transformed into sulfide under the typical operating conditions [6]. Nonetheless, transition metal phosphides belong to a group of catalysts which display excellent activity for hydrodesulfurization (HDS) and hydrodenitrogenation (HDN) reactions [4,5], being the real alternative to sulfides in hydrotreating conditions. Several reviews have been devoted to the synthesis methods, nature, structure and activity of transition metal phosphides [5,6]. Thus, the metal-rich MP or M_2P (M = transition metal) compounds have metallic properties. They combine the properties of metals and ceramics, and thus are good conductors of heat and electricity, are hard and strong, and have high thermal and chemical stability [7].

Several research groups have investigated the synthesis and performance of transition metal phosphide catalysts. Using several metallic phosphides, Oyama [4] concluded that the activity for HDS of DBT and HDN of Q follows the order: $Fe_2P < CoP < MoP < WP < Ni_2P$. The Ni_2P/SiO_2 catalyst exhibits better hydrotreating activity than the traditional $NiMoS/Al_2O_3$ and

* Corresponding author. Tel.: +34 95 213 18 76; fax: +34 95 213 20 00.
** Corresponding author.
E-mail addresses: ainfantes@icp.csic.es (A. Infantes-Molina), ajimenezl@uma.es (A. Jiménez-López).

0926-3373/$ – see front matter © 2011 Elsevier B.V. All rights reserved.
doi:10.1016/j.apcatb.2011.11.022

$CoMoS/Al_2O_3$ systems and it is also efficient in the presence of aromatics and N-containing compounds, which are common inhibitors in the HDS reaction catalysed by sulfides. Stinner et al. [8] prepared six transition metal phosphide catalysts (Co_2P, Ni_2P, MoP, WP, CoMoP, NiMoP) that were tested in the HDN reaction of o-propylaniline. They concluded that the cobalt phosphides, Co_2P and CoMoP, were the least active; Ni_2P and NiMoP displayed an intermediate behaviour, meanwhile MoP and WP were the most active, being the MoP catalyst the most active one. Moreover, Li et al. [9] reported that MoP is less active than the traditional Ni-Mo/Al_2O_3 sulfide catalyst but still more active in the HDN of Q.

The activity trend found in the literature is that MoP-based catalysts present a lower HDS capability than other phosphides but higher than traditional sulfides, while presenting a higher activity in HDN reactions [10–12]. In this regard, Phillips et al. [10] found that a molybdenum phosphide catalyst supported on silica (MoP/SiO_2) was four times more active than a MoS_2/SiO_2 catalyst in the HDS of thiophene after 150 h on-stream. Similarly, Montesinos-Castellanos et al. [11] observed that MoP/Al_2O_3 catalyst turned out to be twice more active in the HDS reaction of DBT than a traditional MoS_2/Al_2O_3 catalyst with the same Mo-loading. Interestingly, it was found that the activity of a MoP catalyst increases progressively with the time on-stream as a consequence of the formation of a phosphosulfide phase, which is reported to be the active phase in phosphide based catalysts [13].

Concerning the preparation, a first study revealed that MoP can be easily obtained by temperature-programmed reduction (TPR) of a metal phosphate precursor [9]. However, novel synthesis methods have been reported to prepare unsupported and supported transition metal phosphides [14–20]. Metal thiophosphates [16] and amorphous alloys [17] precursors, citric acid modified precursors [18], solvothermal synthesis methods [19], novel reducing agents [20] among others have been used. In general, most of these methods yield a high dispersion of supported phosphides. Despite recent advances in the synthesis methods [14,15 and references within] of phosphides, a number of unanswered questions remain. For instance, understanding of factors that govern HDS activity of transition metal phosphides, and the role played by nanoparticles are a few points in the search of metal phosphides for hydrotreating reactions. Accordingly, this work was undertaken with the aim to provide some explanations to the above questions by preparing silica-supported MoP catalysts having nanoparticles of varying size.

In general, the TPR method has been the preferred option to prepare transition metal phosphides. In this method, supported metal phosphides are prepared by impregnating the support with the corresponding metallic precursor salt and ammonium monohydrogenphosphate ($(NH_4)_2HPO_4$, followed by calcination step to develop the oxidic precursor, and finally reduction under hydrogen at high temperature to form the desired phosphide [4]. However, the TPR method itself is poorly suited for alumina-supported phosphide catalysts, because of the high reactivity of alumina toward phosphate, generating aluminium phosphate [15]. In this sense, the use of silica as a support instead of alumina has been explored [21–23]. Moreover, hydrogen reduction of transition metal phosphates typically requires high temperature, upwards of 580 °C to reduce phosphate species due to the P–O bond strength. Recently, with the goal to enhance the traditional catalyst preparation method, a new synthetic approach for nickel and cobalt phosphide-based catalysts was developed in our laboratory [21–23]. In this new synthesis method, the phosphate based precursors are substituted by nickel(II) or cobalt(II) hydrogenphosphite ($Ni(HPO_3H)_2$ or $Co(HPO_3H)_2$) as precursor salts to form the corresponding phosphide. Moreover the catalysts prepared by this new method were found to be active and stable in the HDS of DBT and also in simultaneous reactions of HDS and HDN. Recently, the effect of the use of different phosphorous sources (H_3PO_4, $(NH_4)_3PO_4$, and $NH_4H_2PO_4$) in the preparation of bulk MoP catalysts was studied by also Gong et al. [24].

To determine how the effect of precursor affects HDS and HDN activities of MoP/SiO_2 catalysts, we have prepared different molybdenum phosphide catalysts employing ammonium molybdate ($(NH_4)_2MoO_4$) and phosphorous acid (H_2PO_3H) as precursors of molybdenum and phosphorous, respectively, instead of ammonium heptamolybdate ($(NH_4)_6Mo_7O_{24}{\cdot}4H_2O$) and ammonium dihydrogenphosphate ($(NH_4)H_2PO_4$) employed in the traditional synthetic route. The main goal is the preparation of MoP based catalysts under softer conditions, i.e., at lower reduction temperature. To this end, a phosphorus precursor with lower oxidation state; the usage of molybdate instead of heptamolybdate as molybdenum precursor; as well as the absence of the calcination step were employed. Moreover the activity of these catalysts has been compared with one prepared by the conventional method presented in the literature.

2. Experimental

2.1. Substrate and reagents

The support used in this study was Cab-o-sil type commercial silica. Ammonium heptamolybdate tetrahydrate, $(NH_4)_6Mo_7O_{24}{\cdot}4H_2O$ (Merck 99%), ammonium dihydrogenphosphate, $(NH_4)H_2PO_4$ (Merck 99%), ammonium molybdate, $(NH_4)_2MoO_4$ (Aldrich 99.98%), and phosphorous acid, H_2PO_3H (Aldrich 99%) were employed as molybdenum and phosphorous precursor salts. The chemical products utilized in the reactivity study were dibenzothiophene (Aldrich 98%) and quinoline (Sigma–Aldrich 98%) in cis-, trans-decahydronaphthalene (Sigma–Aldrich 98%). The gases employed were He (Air Liquide 99.99%), H_2 (Air Liquide 99.999%) and N_2 (Air Liquide 99.9999%).

2.2. Preparation of catalysts

2.2.1. Conventional method

A Cab-o-sil type commercial silica was used as a support of MoP-based catalyst (15 wt% of Mo) prepared by the conventional method. The preparation of the catalyst was carried out following the incipient wetness impregnation method by adding the desired amounts of ammonium heptamolybdate tetrahydrate, $(NH_4)_6Mo_7O_{24}{\cdot}4H_2O$, and ammonium dihydrogenphosphate, $(NH_4)H_2PO_4$, to the incipient volume. The impregnated solid was dried at 60 °C, and then calcined in air at 550 °C (1 °C min^{-1}) for 6 h, obtaining so the corresponding catalyst precursor. Finally, the precursor was reduced from 100 °C to 700 °C (2 °C min^{-1}) under a H_2 flow of 100 mL min^{-1}. The precursor and reduced catalyst prepared by this method will be referred to as MoP-c and MoP-c/r700, respectively; c/r refers to calcinated/reduced. Prior to the reduction, all the samples were treated with a He flow of 60 mL min^{-1} for 1 h at 100 °C.

2.2.2. Novel method

A novel MoP/SiO_2 catalyst was also prepared using Cab-o-sil type commercial silica as a support. The preparation of the catalyst was carried out following the incipient wetness impregnation method by adding the desired amounts of ammonium molybdate, $(NH_4)_2MoO_4$, and phosphorous acid, (H_2PO_3H), to the incipient volume. Equimolar amounts of molybdenum and phosphorous salts were used to obtain 15 wt% of MoP. Once the aqueous salt precursor solution was added to the pelletized support (0.85–1.00 mm), the impregnated solid was air dried. Finally, temperature programmed reduction with hydrogen was used to develop the MoP phase. In

this sense, the sample was placed in a tubular quartz reactor, heating at linear temperature ramp (3 °C min^{-1}) in flowing hydrogen (100 mL min^{-1}) from 100 °C to the corresponding reduction temperature, i.e., 550 °C, 600 °C and 700 °C. The precursor and reduced catalyst prepared by this method will be referred to as MoP-d, and MoP-d/rT*r*, respectively; being T*r* the reduction temperature in °C and d/r refers to dried/reduced.

2.3. Characterization of catalysts

Metal contents of reduced catalysts were determined by atomic absorption spectrophotometry using a Perkin-Elmer Optima 3300 DV inductively coupled plasma atomic emission spectrometer (ICP-AES). The solid samples were first digested (in a mixture of HF, HCl and HNO_3) in a microwave oven at a maximum power of 650 W for 2 h, and then aliquots of solution were diluted to 50 mL using deionized water (18.2 mΩ quality).

The temperature programmed reduction of metal phosphite/phosphate to metal phosphide was carried out by placing 80 mg of catalyst precursor in a quartz tubular reactor, with heating at a linear temperature ramp (3 °C min^{-1}) in flowing H_2 (100 mL min^{-1}) from 100 to 800 °C. The evolved gases were sampled in a quadrupole mass spectrometer Balzers GSB 300 02 equipped with a Faraday detector (0–200 uma), and the masses 2 (H_2), 18 (H_2O), and 34 (PH_3) were monitored during the experiment. These signals and temperature were recorded in real time by an on-line computer.

X-ray diffraction patterns (XRD) of the precursor, reduced and spent catalysts were obtained with a X'Pert Pro MPD Philips diffractometer (PANanalytical), using monochromatic CuKα radiation (λ = 1.5406 Å). The Kα radiation was selected with a Ge(1 1 1) primary monochromator. The X-ray tube was set at 45 kV and 40 mA.

The fresh and spent catalysts were studied by HRTEM microscopy using a JEM 2100F microscope operating with a 200 kV accelerating voltage and fitted with an INCA X-sight (Oxford Instruments). The samples were ground into a fine powder and dispersed ultrasonically in hexane at room temperature. Then, a drop of the suspension was put on a lacey carbon-coated Cu grid. At least ten representative images were taken for each sample. In order to obtain statistically reliable information, the length of ca. 500 particles was measured. Particle size distribution was evaluated from several micrographs taken from the same sample.

The textural properties (S_{BET}, V_p, d_p) of the reduced catalysts were obtained from the N_2 adsorption–desorption isotherms at −196 °C measured with a Micromeritics ASAP 2020 apparatus. Prior to the measurements, the samples were degassed at 200 °C and 10^{-4} mbar overnight. Surface areas were determined by using the Brunauer–Emmet–Teller equation [25] and a nitrogen molecule cross section of 16.2 Å^2. The pore size distribution was calculated by applying the Barrer–Joyner–Halenda (BJH) method to the adsorption branch of the N_2 isotherm. The total pore volume was calculated from the adsorption isotherms at $P/P_0 = 0.98$.

The acidity of the fresh reduced catalysts prepared was determined by temperature-programmed desorption (TPD) of ammonia measurements carried out in a Micromeritics TPR/TPD 2900 instrument. Before ammonia adsorption, a sample (0.03 g) was *in-situ* pre-reduced in the TPD cell at 550 °C, 600 °C or 700 °C (heating rate = 3 °C min^{-1}) in a stream of 5%H_2/Ar, cooled down in He flow to 100 °C, and then exposed to ammonia for 0.5 h. TPD measurements were started from 100 °C at a heating rate of 15 °C min^{-1} till 1000 °C using helium as a carrier gas (50 mL min^{-1}). In order to determine the total acidity of the catalyst from its NH_3 desorption profile, the area under the curve was integrated. A semiquantitative comparison of the strength distribution was achieved by Gaussian deconvolution of the peaks. Weak, medium and strong acidities were defined as the areas under the peaks at the lowest, medium and highest temperatures, respectively.

X-ray photoelectron spectra were collected using a Physical Electronics PHI 5700 spectrometer with non-monochromatic Al Kα radiation (300 W, 15 kV, and 1486.6 eV) with a multi-channel detector. Spectra of pelletized samples were recorded in the constant pass energy mode at 29.35 eV, using a 720 μm diameter analysis area. Charge referencing was measured against adventitious carbon (C 1*s* at 284.8 eV). A *PHI ACCESS ESCA-V6.0 F* software package was used for acquisition and data analysis. A Shirley-type background was subtracted from the signals. Recorded spectra were always fitted using Gaussian–Lorentzian curves in order to determine the binding energies of the different element core levels more accurately. Reduced and spent catalysts were stored in sealed vials with an inert solvent. The sample preparation was done in a dry box under a N_2 flow, where the solvent was evaporated prior to its introduction into the analysis chamber, and directly analyzed without previous treatment.

Elemental chemical analysis was performed for spent catalysts with a LECO CHNS 932 analyzer to determine the sulfur and the nitrogen content present after the catalytic test through the combustion of the samples at 1100 °C in pure oxygen to form NO and SO_2.

2.4. Catalytic activity

For the catalytic tests, the HDS of DBT and the HDN of Q were chosen, which were performed in a high-pressure fixed-bed continuous-flow stainless steel catalytic reactor (9.1 mm in diameter, and 230 mm in length), operated in the down-flow mode. The reaction temperature was measured with an interior placed thermocouple in direct contact with the catalyst bed. The organic feed was adjusted to solutions in cis-, trans-decahydronaphthalene of: DBT (3000 ppm) for the study of HDS reaction, Q (3000 ppm) for the study of HDN reaction, 3000 ppm DBT + 200 ppm Q for the study of HDS + (N) and 3000 ppm Q + 200 ppm DBT for the study of HDN + (S) as competitive reactions.

Each solution was supplied by means of a Gilson 307SC piston pump (model 10SC). For the activity tests, 0.5 g of catalyst was used (particle size 0.85–1.00 mm) and was diluted with silicon carbide to 3 cm^3. Prior to the activity test, the catalysts were reduced *in situ* at atmospheric pressure with a H_2 flow of 100 mL min^{-1} by heating from r.t. to 550 °C, 600 °C or 700 °C at a heating rate of 3 °C min^{-1}. Catalytic activities were measured at different temperatures (300–475 °C), under 3.0 MPa of H_2, with a flow rate of 100 mL min^{-1} and with hourly space velocities (WHSV) of 32 h^{-1}. Moreover, the stabilities of the catalysts were studied at a constant temperature reaction for 1800 min. The evolution of the reaction was monitored by collecting liquid samples after 1 h at the desired reaction temperature. These liquid samples were kept in sealed vials and subsequently analyzed by gas chromatography (Shimadzu GC-14B, equipped with a flame ionization detector and a capillary column, TBR-14, coupled to an automatic Shimadzu AOC-20i injector).

For these catalysts, the main HDS products of the reaction were biphenyl (BP), cyclohexylbenzene (CHB), bicyclohexyl (BCH), benzene (B) and cyclohexane (CH). The total HDS conversion was calculated from the ratio of converted dibenzothiophene/initial dibenzothiophene. The selectivity of the different reaction products was calculated considering BP, CHB, B and CH as the reaction products.

The specific activity related to MoP/Si atomic ratio, *rate* (mol_{DBT} g^{-1} s^{-1}) was calculated according to the Eq. (1):

$$rate = \frac{(F/W) \times x}{MoP/Si} \quad (1)$$

Table 1
Chemical analysis (molar ratio)[a] and textural properties[b] of the pure support and reduced MoP/SiO_2 catalysts.

Sample	Precursors/calcination/reduction	Mo/P	S_{BET} (m^2/g)	V_p (cm^3/g)	d_p[b] (nm)
Silica Cab-o-sil	–	–	215	0.70	8.8
MoP-d/r550	$(NH_4)_2MoO_4/H_2PO_3H$ dried TPR = 100–550 °C	1.08	144	0.42	8.1
MoP-d/r600	$(NH_4)_2MoO_4/H_2PO_3H$ dried TPR = 100–600 °C	1.07	102	0.21	5.9
MoP-c/r700	$(NH_4)_6Mo_7O_{24}{\cdot}4H_2O/(NH_4)H_2PO_4$ calcined at 550 °C TPR = 100–700 °C	1.12	47	0.10	5.8

[a] As determined by ICP.
[b] As determined by N_2 physisorption at −196 °C; S_{BET}: specific BET surface area; V_p: total pore volume; and d_p: pore diameter calculated by BJH method.

in which, F is the feed rate of dibenzothiophene (mol min^{-1}), W is the catalyst weight (g), x is the fractional conversion and MoP/Si is the atomic ratio obtained from XPS.

In the case of HDN, the main products were 1,2,3,4-tetrahydroquinoline (THQ-1), 5,6,7,8-tetrahydroquinoline (THQ-5), propylcyclohexane (PCH), propylbenzene (PB) and decahydroquinoline (DHQ). The total HDN conversion was calculated:

$$HDN_{Conv.}(\%) = \frac{(C_{Q.Init.} - C_{Q.Final} - C_{Int.Hyd.})}{C_{Q.Init.}} \times 100$$

where $C_{Q.Init.}$ represents the quinoline concentration in the feed, $C_{Q.Final}$ is the quinoline concentration in the HDN liquid product and $C_{Int.Hyd.}$ is the concentration of hydrogenated intermediates (THQ-1, THQ-5 and DHQ). The selectivity was calculated considering PCH, PB, DHQ, THQ-1 and THQ-5 as products of HDN reaction. Moreover we have only observed slight traces of some unknown compounds in a few cases.

3. Results and discussion

3.1. Catalyst characterization

3.1.1. Elemental analysis

Table 1 reports the molybdenum and phosphorus contents of the reduced catalysts as determined by ICP-AES technique and expressed as Mo/P molar ratio. As seen in this table, all the catalysts prepared possess Mo/P molar ratios close to the nominal one (1).

3.1.2. Structural characterization by H_2-TPR

The formation of MoP phase by the two synthetic approaches was carried out by H_2-TPR method. The reaction was monitored by a quadrupole mass spectrometer, following the evolution of the H_2O (m/z = 18) and PH_3 (m/z = 34) signals during the reduction process; these profiles are depicted in Fig. 1. Despite the fact that the reduction profiles show a similar tendency for both catalysts, the precursor prepared following the conventional method (MoP-c) shows profile with the maximum shifted to higher temperatures. This is a consequence of the difficulty to reduce both phosphate and heptamolybdate employed in the traditional method (reduction of calcined precursor) with regards to phosphite and molybdate used in the new method (reduction of dried precursor). Considering the explanation of the MoP formation by temperature-programmed reduction proposed by Yang et al. [26], PH_3 is formed and then reacts with the surface molybdenum particles to form P-atoms that are chemisorbed on these Mo particles forming a thin film of MoP*x*.

The water profiles (Fig. 1(A)) indicate the occurrence of several processes, depending on the precursor employed. The dried precursor shows a slight water loss at low temperatures, from 150 °C to 300 °C, due to the release of physisorbed water [27], and another one at higher temperatures originated likely from the reduction of the precursor to form the MoP active phase (T > 375 °C) [28]. The calcined substrate, prepared by the conventional method, does not show the component of physisorbed water probably due to the removal of molecular water under the mild pre-treatment with He at 100 °C. At higher temperatures, three overlapped peaks (α, β and γ) appear. The same three peaks have been observed by Clark and Oyama [28] in the TPR profile of a MoP/Al_2O_3 catalyst. The first one (α) at ca. 450 °C has been assigned to dehydroxylation of

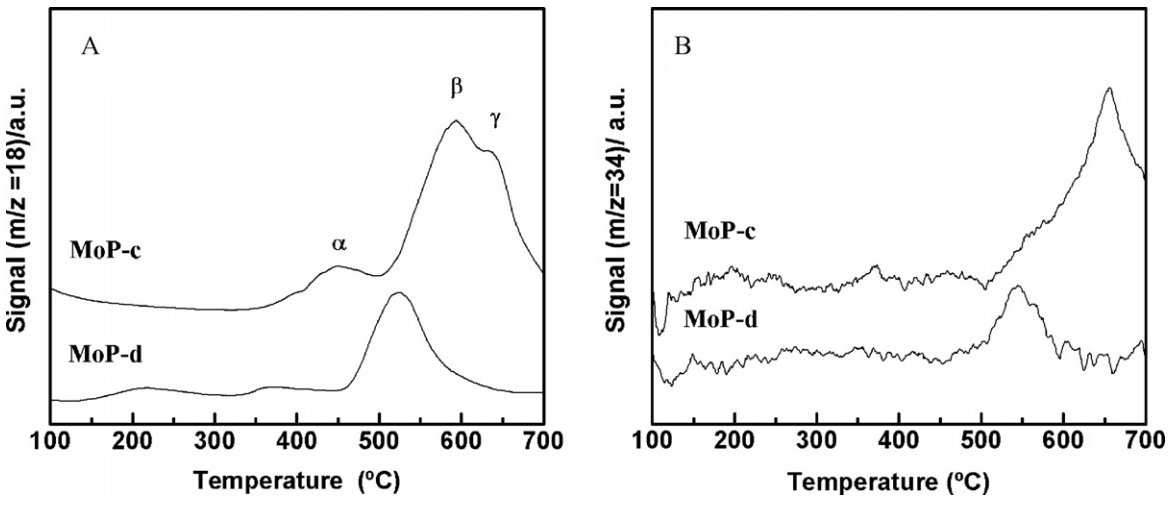

Fig. 1. Mass 18 (H_2O) and 34 (PH_3) signals obtained during temperature-programmed reduction of MoP/SiO_2 substrates.

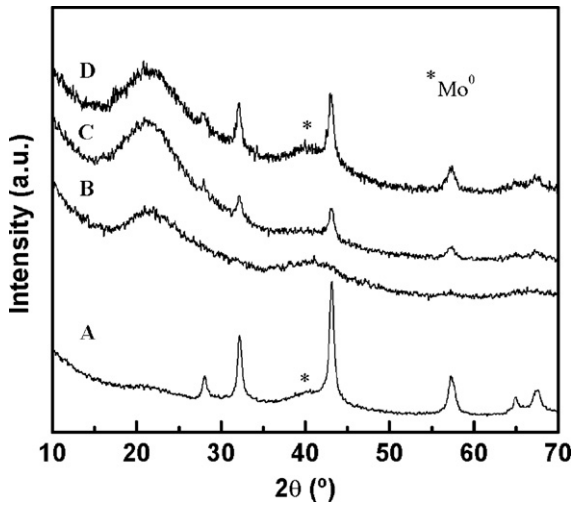

Fig. 2. X-ray diffraction patterns of reduced catalysts: (A) MoP-c/r700; (B) MoP-d/r550; (C) MoP-d/r600; and (D) MoP-d/r700.

well-dispersed molybdate species; while the β and γ peaks correspond to $MoO_3 \rightarrow MoO_2$ and $MoO_2 \rightarrow Mo^0$ reduction processes, respectively. Molybdenum metal then reacts with phosphine to form the MoP phase [27–29]. The calcined sample shows the peaks of water formation at higher temperature indicating higher reduction temperature required to form the MoP phase.

The PH_3 signal (Fig. 1(B)) only shows a single component at temperatures higher than 500 °C that is related with the β process of water released (Fig. 1(A)) indicating that the release of water and phosphine at this temperature are related to the same reduction process to form the MoP phosphide [29]. The PH_3 desorption occurs at lower temperature with the MoP-d sample indicating the better reducibility of this sample as expected according to the precursor salts employed. The PH_3 component at 500 °C indicates that this temperature could be appropriate to reduce phosphite species.

3.1.3. Crystalline structure

The formation of crystalline phases was verified by X-ray powder diffraction. The 15 wt% Mo precursor did not show diffraction lines, only a broad band between $2\theta = 20$ and 30° originated by amorphous silica is visible. The influence of the reduction temperature on the formation of the MoP phase for the catalyst prepared by the new method is depicted in the B–D patterns of Fig. 2. It can be seen that in so far as the reduction temperature increases the diffraction lines of the MoP phase do, i.e., the formation of more MoP and more crystalline happens (*vide infra*). Except the catalyst prepared by the new method and reduced at 550 °C, all the catalysts exhibit the diffraction lines arising from the MoP phase (PDF Card N° 03-065-6487) located at $2\theta = 27.9, 32.0, 43.0, 57.1, 64.8$ and 67.6° corresponding to (0 0 1), (1 0 0), (1 0 1), (1 1 0), (1 1 1) and (1 0 2) reflexions, being the main diffraction signal located at $2\theta = 43.0$°. At 550 °C, the diffraction lines are not noticeable although the presence of the MoP phase cannot be discarded as it will be seen in XPS analysis. Besides, from H_2O and PH_3 profiles in the H_2-TPR experiment it could be expected that at 550 °C the formation of MoP phase should be happening. On the other hand, by comparing the patterns of the catalysts reduced at the same temperature (700 °C) and prepared by different methods (Fig. 2(A) and (D)), it can be seen how the catalyst prepared by the conventional one displays well defined and more intense diffraction lines. Therefore, it can be concluded that the new synthetic approach favours the formation of smaller and more dispersed MoP crystallites. Moreover, regardless of the catalyst preparation method employed, the patterns of the catalysts reduced at 700 °C (Fig. 2(A) and (D)), shows a broad and tiny shoulder at ca. $2\theta = 40.5$° associated with the main diffraction line of Mo^0 (PDF Card N° 00-042-1120), indicating that at this reduction temperature metallic Mo is formed on the catalyst surface.

From the results presented above and with the main objective of diminishing the reduction temperature used in the traditional method, reduction temperatures of 550 °C and 600 °C have been used to activate catalysts prepared by reduction of dried precursor prior to catalytic testing. The reduction temperatures selected here are close to that employed by Clark and Oyama [28] for silica-supported MoP (577 °C) and Montesinos-Castellanos et al. [30] for alumina-supported MoP (550 °C), although they maintained the catalysts for 2 h at this reduction temperature. The preparation method exposed here does not require such a reduction isotherm.

3.1.4. Morphology analysis (TEM)

TEM analysis of reduced catalysts was used with the aim to elucidate the distribution of the active phase. The micrographs corresponding to MoP-d/r550, MoP-d/r600 and MoP-c/r700 catalysts are shown in Fig. 3(A)–(C), respectively. Regardless of the reduction temperature (550 versus 600 °C), the two catalysts prepared from dried precursors show well-defined and smaller MoP particles than the sample prepared by reduction of calcined precursor. The MoP particles supported on silica adopted a globular morphology, as observed by other authors [4,10,31,32]. The influence of the catalyst preparation methodology on the particle size distribution can be deduced from Fig. 3(D) which shows the histograms of the fresh reduced catalysts. The two catalysts prepared from dried precursors show narrower particle size distributions than the catalyst prepared by the conventional method. The average size of MoP particles follows the trend: MoP-c/r700 (6.5 ± 1.5 nm) ≫ MoP-d/r600 (2.1 ± 0.2 nm) > MoP-d/r550 (1.3 ± 0.2 nm). Thus, the catalysts prepared by the new synthetic approach present well-defined and small particles highly dispersed on the support. As one could expect from a lower reduction temperature [12], the catalyst reduced at 550 °C shows lower particle size than that reduced at 600 °C.

To conclude, in good agreement with the above XRD data, TEM results indicated the best active phase dispersion on MoP-d/r550. In other words, the new preparation method provides catalysts with a better dispersion of the active phase obtained at a lower reduction temperature. The comparison of the histograms of spent catalysts prepared by this method (not shown here) with those of fresh catalysts indicated that the particle size was preserved during on-stream conditions.

3.1.5. Textural properties

The textural properties of the catalysts were evaluated from the N_2 adsorption–desorption isotherms at −196 °C and the corresponding data are compiled in Table 1. In Fig. 4 the N_2 adsorption–desorption isotherms of the MoP catalysts prepared by the two methods and reduced at different temperatures are compared with the naked support (silica Cab-o-sil). There are no changes in the isotherm type and hysteresis loop after the molybdenum deposition followed by catalyst reduction at different temperatures. According to the IUPAC classification [33], the N_2 isotherms of all the samples are of type II and show a clear H3-type hysteresis loop characteristic of aggregates or agglomerates of particles forming slit shaped pores with non-uniform size and/or shape [34]. Regardless of the reduction temperature, all MoP catalysts supported on silica Cab-o-sil are mesoporous materials with complete absence of micropores. The nitrogen uptake progressively decreases in the whole range of relative pressures with an increase of catalyst reduction temperature from 550 °C to 700 °C (Fig. 4) due to the enhancement of the pore blocking by MoP particles. In line with this, TEM micrographs of MoP catalysts supported on silica Cab-o-sil show an increase of MoP crystal sizes with an

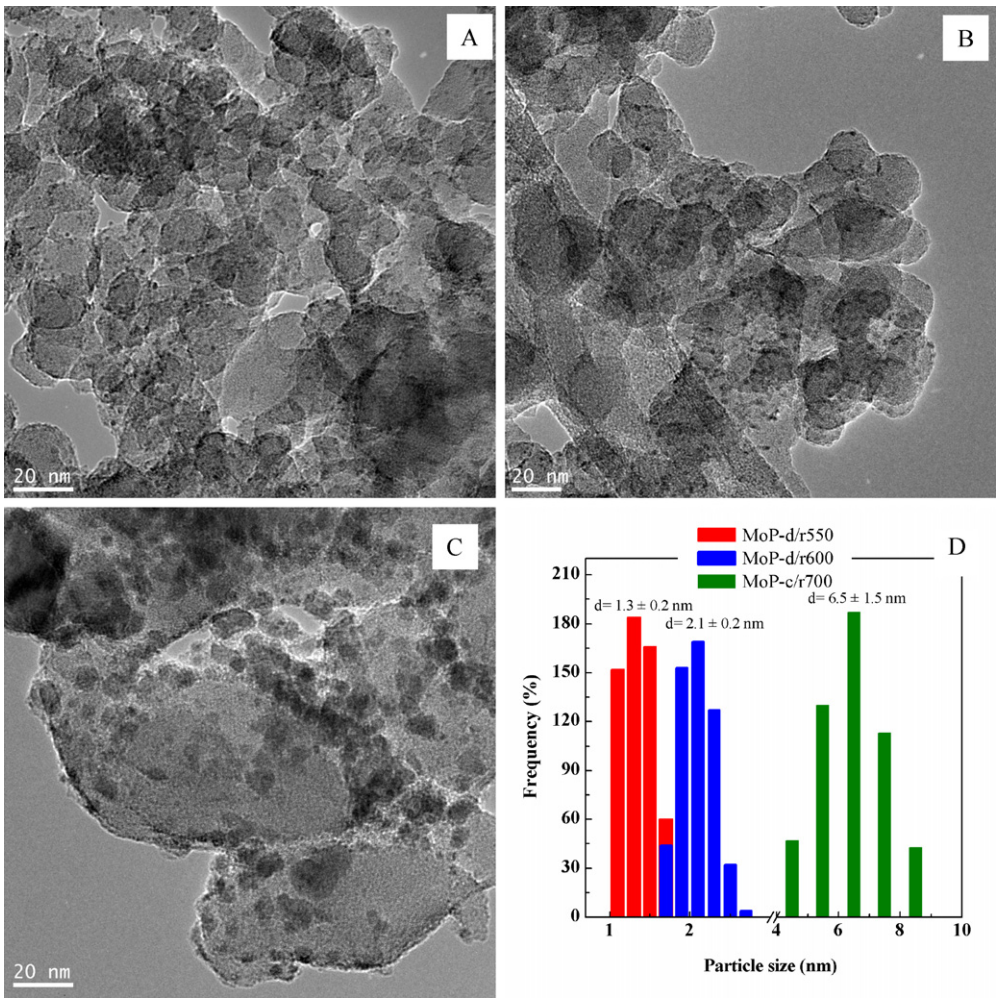

Fig. 3. HR-TEM micrographs of fresh reduced MoP/SiO_2 catalysts prepared by different methods: (A) MoP-d/r550; (B) MoP-d/r600; (C) MoP-c/r700; and (D) histograms of the MoP particle size distribution of all catalysts.

increase of catalyst reduction temperature. The comparison of the isotherms of naked silica and MoP catalysts revealed a considerable shift in the relative pressure of the desorption step indicating the formation of new mesopores after molybdenum loading followed by temperature-programmed reduction.

The specific BET area follows the trend: naked Cab-o-sil silica ($215\,m^2\,g^{-1}$) > MoP-d/r550 ($144\,m^2\,g^{-1}$) > MoP-d/r600 ($102\,m^2\,g^{-1}$) > MoP-c/r700 ($47\,m^2\,g^{-1}$). Thus, almost a five times decrease of specific BET area is observed during the molybdenum deposition and catalyst reduction at 700 °C with respect to the naked Cab-o-sil silica. In line with this, the average pore diameter of 8.1 nm in MoP-d/r550 catalyst decreases to 5.8 nm in MoP-c/r700 catalyst. Similarly, pore volume is also reduced from 0.42 (MoP-d/r550) to $0.10\,cm^3\,g^{-1}$ (MoP-c/r700), as shown in Table 1.

Summarizing, irrespective of the catalyst preparation method, the specific area drops in all cases after the incorporation of the precursor salts. This trend is more evident in samples prepared by the conventional method (reduction of calcined precursor). The catalyst prepared by the new method and reduced at lower temperature, MoP-d/r550, present higher BET areas and pore volumes than the ones prepared by the conventional methodology. Considering HRTEM results (*vide supra*), this is because of the great dispersion of MoP phase achieved in this catalyst.

3.1.6. Surface acidity

The influence of the preparation method as well as the catalyst reduction temperature on the acidity of silica-supported MoP catalysts was deduced from TPD of ammonia. Fig. 5 shows typical plots of ammonia desorption as a function of temperature. The strength of the acid sites can be determined by the temperature at which the adsorbed NH_3 starts to desorb. Based on the desorption temperature, the acid sites were classified as weak ($T < 250$ °C), medium ($T = 250–500$ °C), or strong ($T > 500$° C). The peaks were mathematically fitted using Gaussian functions. As seen in Fig. 5, regardless of reduction temperature, all MoP catalysts showed weak, medium, and strong acid sites. The TCD signal at the highest desorption temperature is more likely due to decomposition of the phosphate phase present on the catalyst surface. The total concentration of acid sites (expressed as $mmol_{NH3}/g_{cat}$) is shown in Table 2. From this table, the total acidity of the catalysts follows the trend: MoP-d/r550 > MoP-d/r600 > MoP-c/r700 indicating that the total acidity of the catalysts decreases with an increase of the reduction temperature from 550 to 700 °C. This is expected taking into account the agglomeration of MoP and dehydroxylation of the support with an increase of the reduction temperature. As a consequence, both catalysts prepared by the novel method showed a larger total acidity than the sample prepared employing the traditional method.

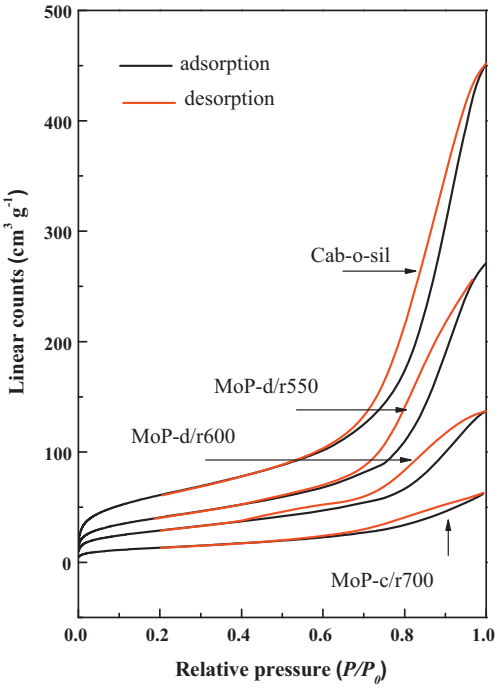

Fig. 4. Comparison of the N_2 adsorption–desorption isotherms of pure support (Cab-o-sil) and reduced MoP/SiO_2 catalysts.

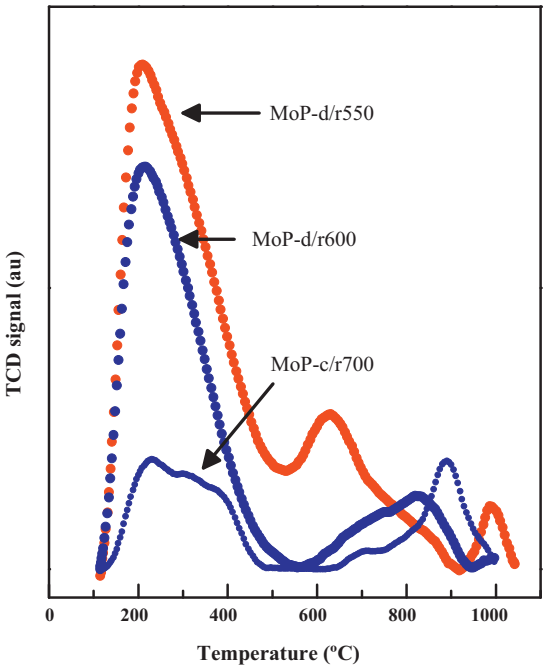

Fig. 5. TPD-NH_3 profiles of reduced MoP/SiO_2 catalysts.

Table 2
Influence of the catalyst preparation method on the acid properties of the reduced MoP/SiO_2 catalysts[a].

Catalyst	Amount of acid sites (mmol NH_3 g_{cat}^{-1})			
	Weak $T<250\,^{\circ}C$	Moderate $T=250–500\,^{\circ}C$	Strong $T>500\,^{\circ}C$	Total
MoP-d/r550	0.28	0.27	0.18	0.72
MoP-d/r600	0.12	0.28	0.08	0.48
MoP-c/r700	0.05	0.08	0.07	0.20

[a] As obtained by Gaussian deconvolution of the TPD-NH_3 patterns.

3.1.7. Surface analysis

For transition metal phosphides hydrotreating catalysts, the primary sites on which reactants adsorb [35], and the electronic state of these sites can be determined by XPS. Mo 3d core-level spectra of the fresh reduced and spent catalysts are shown in Fig. 6. The binding energies of the most intense photoelectron Mo 3d (Mo $3d_{5/2}$) and P 2p (P $2p_{3/2}$) peaks are compiled in Table 3. The Mo 3d core-level spectra for reduced catalysts prepared by the new method (MoP-d/r550 and MoP-d/r600) can be fitted into three doublets with the $3d_{5/2}$ (solid) and $3d_{3/2}$ (dotted) components coming from the spin-orbit splitting. The observation of three doublets indicates that there is more than one kind of molybdenum species. The Mo $3d_{5/2}$ component centred at ca. 227.6 eV is assigned at $Mo^{\delta+}$ surface site forming MoP, lower than the value reported by Phillips et al. [10] for a MoP/SiO_2 system. The Mo $3d_{5/2}$ component at 229.7 eV comes from the presence of partially reduced Mo^{5+} and/or Mo^{4+} species [36]. The last Mo $3d_{5/2}$ contribution at 231.6 eV arises from non-reduced Mo^{6+} species, revealing what was suggested before, a total reduction has not been achieved. The Mo 3d core level spectra of MoP-c/r700 catalyst also present a Mo $3d_{5/2}$ component at 228.1 eV assigned to Mo^0 species [37], which is in accordance to the results obtained by XRD.

The P 2p core-level spectra (not shown here) present three contributions in the form of doublets (P $2p_{3/2}$ and P $2p_{1/2}$ components), being the P $2p_{3/2}$ components located at ca. 129.0, 133.4 and 134.0 eV. The binding energy at 129.0 eV is close to that reported for $P^{\delta-}$ species which are present in phosphides and revealing the formation of such a compound. The second P $2p_{3/2}$ value at 133.4 eV is reported to be due to unreduced HPO_3H^- species from the

Table 3
Spectral parameters and surface atomic ratios of precursors, reduced and spent MoP/SiO_2 catalysts obtained by XPS analysis.

Sample	Binding Energy (eV)							Superficial atomic ratio	
	Mo $3d_{5/2}$				P $2p_{3/2}$			Mo/P	Mo/Si
	Mo^{6+}	Mo^{4+} Mo^{5+}	Mo^0 MoS_2	MoP	HPO_3H^-	PO_4^{3-}	MoP		
Precursors									
MoP-c	232.4	–	–	–	–	133.4	–	0.83	0.25
MoP-d	231.6	231.1	–	–	133.3	134.8	–	0.61	0.02
MoP/SiO_2 catalysts									
MoP-d/r550	231.6	229.7	–	227.7	133.5	133.8	129.4	0.32	0.01
MoP-d/r600	231.6	229.7	–	227.6	133.3	134.2	129.2	0.48	0.01
MoP-c/r700	232.1	230.6	228.1	227.0	–	133.4	128.3	0.89	0.29
Spent catalysts tested in HDS of DBT at 425 °C									
MoP-d/r550	232.3	230.6	229.3	228.3	133.4	134.7	128.5	0.29	0.01
MoP-d/r600	232.3	230.4	228.9	227.7	133.3	134.4	128.5	0.46	0.02
MoP-c/r700	232.3	231.3	229.2	227.8	–	133.5	128.9	1.17	0.21

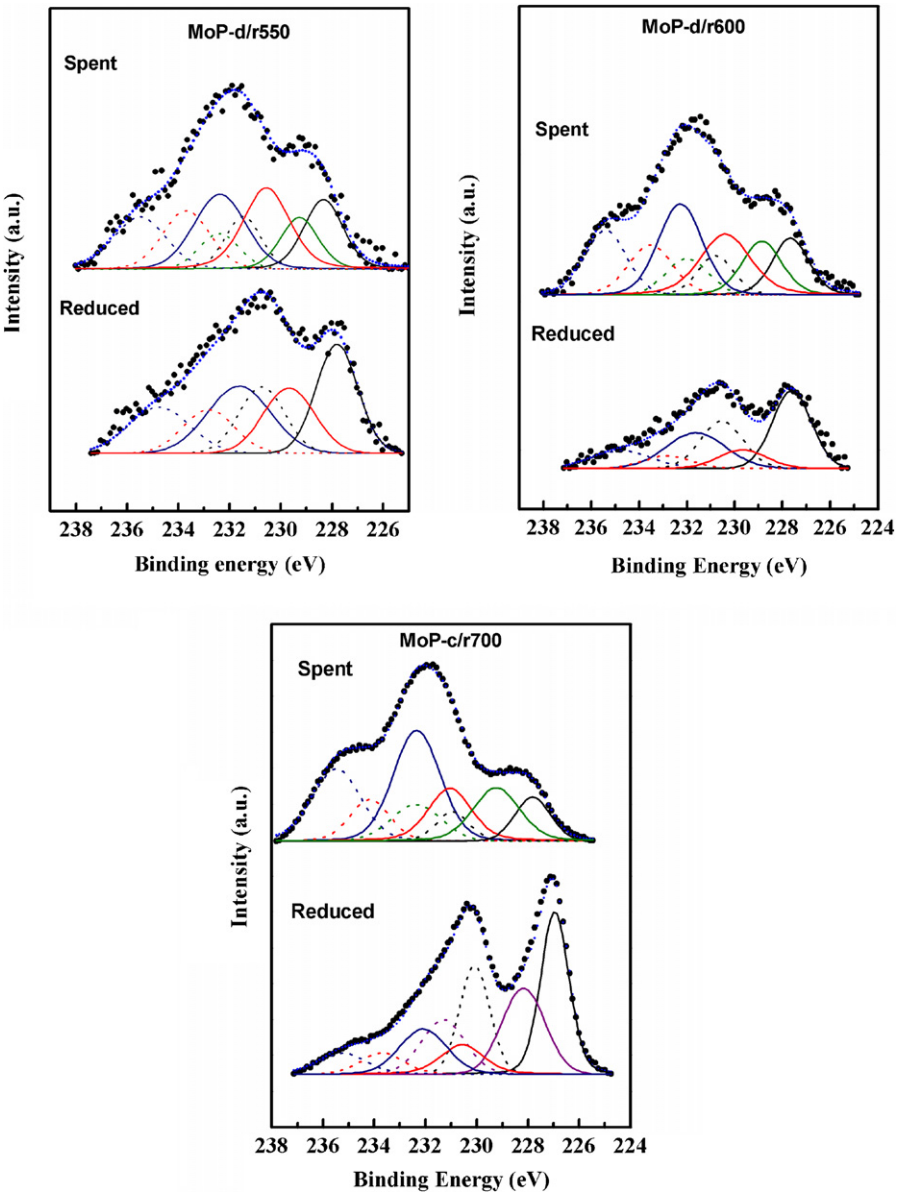

Fig. 6. Mo 3d spectra of fresh reduced and spent MoP/SiO_2 catalysts tested in HDS of DBT reaction at different temperatures. Black contribution: MoP; green contribution: MoS_2-type active site; purple contribution: Mo^0; red contribution: Mo^{5+}/Mo^{4+}; and blue contribution: Mo^{6+}. (For interpretation of the references to color in this figure legend, the reader is referred to the web version of the article.)

precursor salt [21], while the last P $2p_{3/2}$ contribution is due to the presence of phosphate [10] coming from the partial passivation of MoP as it has been observed from Mo 3d core level spectra.

The quantitative XPS analyses of the reduced and spent catalysts are shown in Table 3. The surface exposure of molybdenum species, derived from the Mo/Si atomic ratios, indicates that the catalysts prepared from phosphorous acid and ammonium molybdate, and by reduction of dried precursor, shows good distribution of the MoP phase across the pore network of the substrate, however active phase enrichment occurs in the catalyst prepared by the traditional method (reduction of calcined precursor). Contrary to the latter sample, the comparison of Mo/Si atomic ratio of the MoP-d/r550 and MoP-d/r600 catalysts before and after on-stream reaction (Table 3) indicates that the surface exposure of MoP species remained unchanged after hydrodesulfurization reaction. This suggests a great stability of those catalysts during on-stream reaction.

3.2. Catalytic study

The catalysts presented here were assayed in the HDS reaction of DBT and in the HDN reaction of Q. The mechanisms of HDS and HDN and the products obtained are showed in Schemes 1 and 2, respectively.

3.2.1. DBT HDS reaction

The catalysts prepared were firstly tested in the HDS of DBT (3000 ppm). Fig. 7(A) compares the specific activities of the catalysts prepared by the two methods at 3.0 MPa of hydrogen pressure and at a reaction temperature of 425 °C. In this sense, Fig. 7(A) plots the specific activity referenced to the amount of superficial MoP phase found by XPS considering the different superficial distribution of the MoP phase on these catalysts. The differences found between the two preparations methods are evident, being the catalysts prepared by reduction of dried precursor much more active in the DBT HDS reaction (Fig. 7(A)) than the MoP-c/r700 catalyst

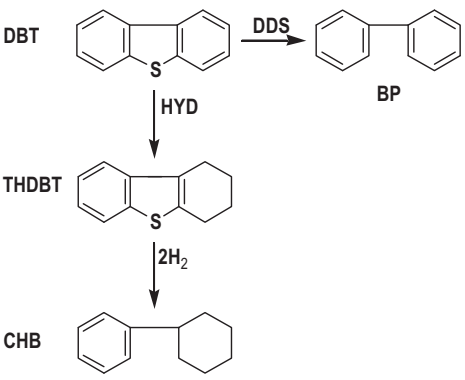

DBT: dibenzothiophene; THDBT: tetrahydrodibenzothiophene; BP: biphenyl; CHB: cylohexylbenzene

Scheme 1. Reaction scheme of HDS of dibenzothiophene (a flow reactor; T = 325–475 °C; P = 3 MPa; WHSV = 32 h^{-1}) over MoP/SiO_2 catalysts: DBT: dibenzothiophene; THDBT: tetrahydrodibenzothiophene; BP: biphenyl; and CHB: cyclohexylbenzene.

prepared by reduction of calcined precursor. With regards to the selectivity to the different reaction products, the HDS reaction of DBT can proceed through two different pathways; a hydrogenation (HYD) route and a direct desulfurization (DDS) route (see Scheme 1). BP and CHB are the main products of the DDS and HYD routes, respectively. BP is the main product obtained here, with selectivity values above 85% in all cases; therefore the reaction pathway seems to go through the DDS route. These data indicate that the reaction pathway is not influenced by the catalyst acidity.

Moreover the stability of the catalysts prepared by the new synthetic approach (MoP-d/r550 and MoP-d/r600) was evaluated during 30 h on-stream at 425 °C of reaction temperature with a feed containing 3000 ppm DBT. Fig. 7(B) and (C) depicts the conversion and selectivity (BP formation) evolutions with the reaction time, respectively. It is observed that an increase in HDS conversion occurs in both cases being MoP-d/r550 a little more active after 30 h of on-stream reaction than its MoP-d/r600 counterpart (DBT conversion about 80%). These results indicate that at 550 °C, enough MoP phase is formed to convert most of DBT molecules. Interestingly, regardless of the reaction time, the former sample shows higher selectivity toward biphenyl formation than the later.

3.2.2. HDS and HDN competitive reactions

MoP-d/r550 catalyst was also studied in simultaneous HDS + HDN reactions: (i) HDS of DBT in the presence of small amount of quinoline (HDS + (N)); and (ii) HDN of quinoline in the presence of small amount of DBT (HDN + (S)). Considering that HDN and HDS reactions take place simultaneously and H_2S is always present as HDS product, it is fully described in the literature that the presence of this compound alters the HDN activity in the same way that Q HDN products could alter the HDS activity.

Fig. 8(A) lumps together the HDS conversion attained by this catalyst by feeding different DBT/Q ratios as a function of the reaction temperature. The HDS conversion Fig. 8(A) of this catalyst reveals that the presence of quinoline in the DBT HDS reaction does not have any influence on the HDS behaviour as long as the catalyst presents the same pattern of conversion at all studied temperatures. With regards to the selectivity pattern presented by this catalyst in both reactions, the HDS reaction proceeds through the DDS route, with a selectivity value to BP higher than 90% in all cases (data not shown here). This fact indicates that HDS reaction is not influenced by the presence of N-containing molecules as it has been observed in the case of Ni_2P and CoP catalysts prepared and tested in a similar way [38] and suggesting that HDS and HDN reactions take place on different active sites and HDN products have no influence on HDS reaction.

In a parallel way, MoP-d/r550 catalyst was assayed in the HDN reaction of Q and studied the influence of the presence of DBT molecules in this reaction. With this aim, two feeds with different DBT/Q ratio were prepared: 3000 ppm Q + 200 ppm DBT (HDN + (S)) and 3000 ppm DBT + 200 ppm (HDS + (N)) and the catalyst tested as a function of the reaction temperature. Fig. 8(B) shows that

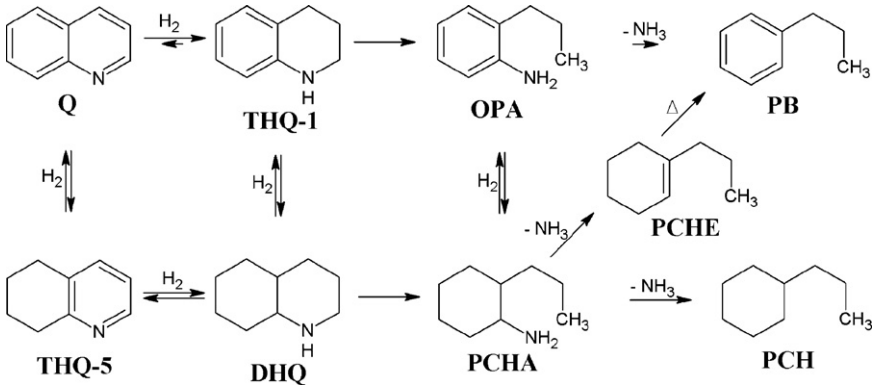

Scheme 2. Reaction scheme of HDN of quinoline (a flow reactor; T = 325–475 °C; P = 3 MPa; and WHSV = 32 h^{-1}) over MoP/SiO_2 catalysts. Q: quinoline; THQ-1: 1,2,3,4-tetrahydroquinoline; OPA: o-propylaniline; PB: propylbenzene; THQ-5: 5,6,7,8-tetrahydroquinoline; DHQ: decahydroquinoline; PCHA: propylcyclohexylamine; PCHE: propylcyclohexene; and PCH: propylcyclohexane.

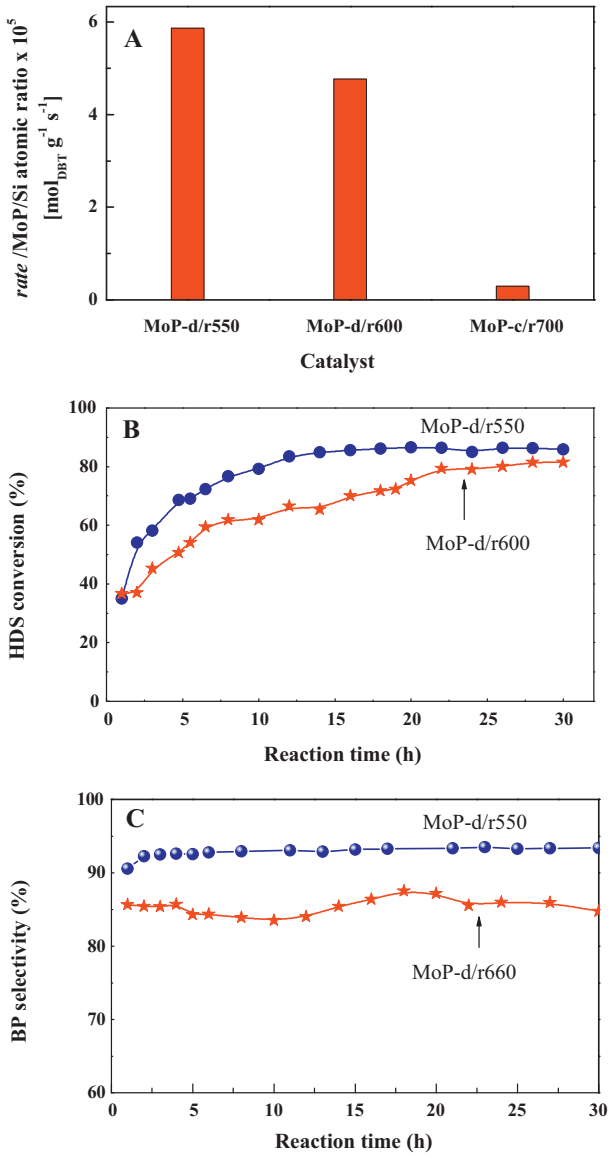

Fig. 7. (A) Comparison of the activities of MoP/SiO_2 catalysts in HDS of DBT (T = 425 °C, P = 3 MPa, WHSV = 32 h^{-1}) after 30 h of on-stream reaction. Influence of the reaction time on DBT conversion (B) and selectivity toward BP formation (C) in the HDS of DBT over MoP-d/r500 and MoP-d/r600 catalysts.

Table 4
Influence of temperature on selectivities toward HDN reaction[a] products for MoP-d/r550 catalyst.

Products	HDN (%)		HDN + (S) (%)		HDS + (N) (%)	
	$T_{325\,°C}$	$T_{475\,°C}$	$T_{325\,°C}$	$T_{475\,°C}$	$T_{325\,°C}$	$T_{475\,°C}$
THQ-1	62.2	16.7	82.3	17.9	49.2	4.5
THQ-5	17.5	50.5	5.0	39.2	15.2	6.5
DHQ	10.3	5.2	6.7	8.8	2.1	1.1
PB	5.2	19.9	4.0	26.8	21.8	68.7
PCH	4.7	7.6	2.1	7.2	11.6	19.3

[a] Reaction conditions were: T = 325 and 475 °C; P = 3.0 MPa; and WHSV = 32 h^{-1}. Feed composition was: HDN: 3000 ppm of Q; HDS + (N): 3000 ppm of DBT + 200 ppm of Q; and HDN + (S): 3000 ppm of Q + 200 ppm of DBT.

MoP-d/r550 catalyst shows a very low activity in the HDN and HDN + (S) reactions (HDN conversion < 20%). For the HDS + (N) reaction, the catalyst presents an activity increase with the reaction temperature, attaining 65% of conversion at 475 °C, i.e., the catalyst is capable of nitrogen removing under the presence of a great amount of DBT molecules. The HDN activity under the presence of sulfur containing molecules is known to be strongly dependent on the reaction temperature: at temperatures higher than 350 °C, the addition of DBT (200 ppm) starts to be beneficial on Q conversion, whereas at low temperatures a contrary effect occurs. A similar effect was observed previously [39] indicating the competitive adsorption of thiophene at low temperatures on hydrogenation sites, which obviously retarded the hydrogenation of pyridine to piperidine. At higher temperatures, H_2S produced in the HDS of thiophene increased the rate of piperidine hydrogenolysis and enhanced the overall HDN reaction rate. Our results are in agreement, pointing to sulfur coming from HDS reaction which favours the HDN reaction. In good agreement with the study of Satterfield et al. [39], a detailed study by Egorova and Prins [40] about the interaction between DBT and 2-methylpyridine (or 2-methylpiperidine) over a sulfided NiMo/Al_2O_3 catalyst strongly suggests that C–N and C–S bond breaking takes place at different active sites, whereas the hydrogenation sites for N- and S-containing molecules may be the same.

With regards to HDN selectivity, contrary to HDS reaction, the selectivity patterns attained in the HDN reaction depend on the Q/DBT ratio fed and the corresponding selectivity values attained at the beginning (325 °C) and the end (475 °C) of the reaction are compiled in Table 4. The HDN of quinoline can proceed via fully hydrogenated intermediates (DHQ-PCHA) or via partially hydrogenated intermediates (THQ-1-OPA) (Scheme 2). In a first step, the hydrogenation of the N-containing ring is easily achieved, and a thermodynamic equilibrium between Q and THQ-1 is readily established under typical HDN conditions. This process is favoured at low temperatures. At moderate temperatures, it has been suggested that HDN of Q mainly takes

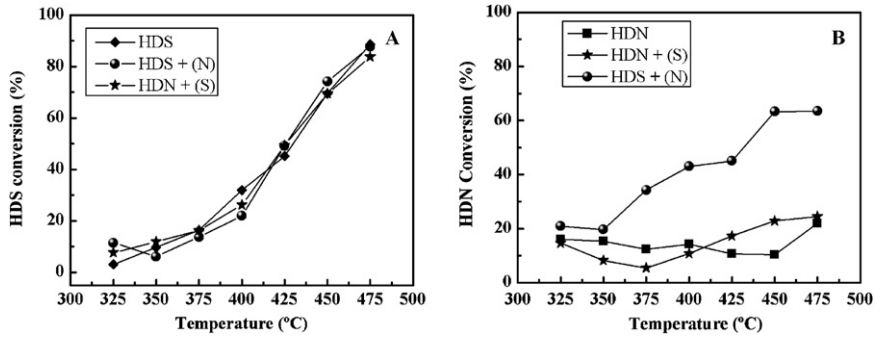

Fig. 8. Influence of temperature on HDS (A) and HDN (B) conversions in simultaneous HDS + (N) and HDN + (S) reactions over MoP-d/r550 catalyst: HDS: 3000 ppm of DBT; HDS + (N): 3000 ppm of DBT + 200 ppm of Q; HDN: 3000 ppm of Q; HDN + (S): 3000 ppm of Q + 200 ppm of DBT.

Table 5
Activity and selectivity in the long-time HDS and HDN reactions[a] over MoP-d/r550 catalyst.

	HDS of DBT			HDN of Q		
	Conversion (%)	BP (%)	CHB (%)	Conversion (%)	PCH (%)	PB (%)
HDS	85.0	93.0	4.3	–	–	–
HDS + (N)	83.2	93.4	4.0	61.9	29.5	49.6
HDN	–	–	–	10.6	9.3	13.0
HDN + (S)	58.2	84.7	15.3	19.2	6.8	11.7

[a] Reaction conditions were: $T = 425\,^{\circ}C$; $P = 3.0$ MPa; WHSV = 32 h^{-1}; and $t = 30$ h. Feed composition was: HDS: 3000 ppm of DBT; HDS + (N): 3000 ppm of DBT + 200 ppm of Q; HDN: 3000 ppm of Q; and HDN + (S): 3000 ppm of Q + 200 ppm of DBT.

place through the fully saturated intermediates (DHQ-PCHA) that results in PCHE which undergoes further (de)hydrogenation to PCH and PB. Nonetheless, the mechanism can also take place through THQ-1 [41] and the hydrogenolysis of the aliphatic C–N bond (CNH) to obtain ortho-propylaniline (OPA). Several authors have established that the reaction of OPA is greatly inhibited by Q and THQ-1, so the partially hydrogenated pathway should be unfavourable by self-inhibiting effect [42]. However, at high temperatures, some authors have reported [43] that the reaction of Q → THQ-1 → OPA → PB is favoured if phosphorus is present on the catalyst surface. So the PCH/PB ratios account for the contribution of the two HDN pathways in the quinoline network. These authors report that both reaction paths are important in the HDN of quinoline.

The products detected here, with the different feeds, are 1,2,3,4-tetrahydroquinoline (THQ-1), 5,6,7,8-tetrahydroquinoline (THQ-5) and DHQ, as hydrogenated intermediates; and PCH and PB as denitrogenated products. The amount of decahydroquinoline detected is only sizeable in the tests with DBT molecules, with selectivity values lower than 10%. In general, at the beginning of the reaction (325 °C) and with low HDN conversion, the hydrogenated intermediate 1,2,3,4-tetrahydroquinoline is the favoured product in all cases. The higher amounts of 1,2,3,4-tetrahydroquinoline are obtained with feeds containing 3000 ppm of Q (HDN) and 3000 ppm Q + 200 ppm DBT (HDN + (S)), 62.2 and 82.3%, respectively, at 325 °C. This product, at higher temperature (475 °C), is transformed into the hydrogenated intermediate 5,6,7,8-tetrahydroquinoline and/or into denitrogenated propylbenzene and propylcyclohexane, being the quantity of each one dependent on the feed tested. In the literature it is reported that by increasing the temperature, 1,2,3,4-tetrahydroquinoline is hydrogenated to decahydroquinoline and in the next step decahydroquinoline leads to 5,6,7,8-tetrahydroquinoline (Scheme 2), more favoured than propylcyclohexane due to kinetic parameters [44]. In this sense, at 475 °C the percentage of 5,6,7,8-tetrahydroquinoline detected in the HDN and HDN + (S) tests is 50.5 and 39.2%, respectively; the percentage of 1,2,3,4-tetrahydroquinoline is close to 17% in both cases and the percentage of decahydroquinoline is 5.2 and 8.8%, respectively. Meanwhile the selectivity to denitrogenated products is ca. 7% for propylcyclohexane and between 20 and 27% for propylbenzene at 475 °C. Nonetheless the catalyst tested in the presence of small amount of quinoline (HDS + (N)) presents very low selectivity (12%) to partially hydrogenated intermediates (THQ-1 + DHQ + THQ-5) while a high selectivity to denitrogenated products such as propylbenzene (68.7%) and propylcyclohexane (19.3%). From these data it can be stated that MoP catalyst is only capable of removing quinoline molecules when they are present in low concentrations, without being inhibited the HDN reaction by the presence of DBT molecules being the main denitrogenated product propylbenzene, coming from the partially hydrogenated intermediates route. Egorova and Prins [40] reported that DBT adsorbs much stronger on the hydrogenation sites than H_2S. This strong adsorption of DBT on hydrogenation sites could be responsible for the tendency of these catalysts of following the DDS route in the HDS reaction and the partially hydrogenated intermediates route in the HDN reaction.

In order to obtain information on the life time of the MoP-d/r550 catalyst, this sample was tested in simultaneous HDS and HDN reactions at 425 °C for 30 h with feeds containing 3000 ppm DBT + 200 ppm Q (HDS + (N)) and 3000 ppm Q + 200 ppm DBT (HDN + (S)). The activity and selectivity data achieved after 30 h for the MoP-d/r550 catalyst are reported in Table 5. The catalyst tested in HDS + (N) presents better HDS and HDN conversion values after 30 h of reaction time. DBT conversion only decays, with regards to a Q free feed (85.0%), when a high concentration of Q is present, HDN + (S) (58.2%). Q conversion was found to be always higher in the presence of DBT, HDN + (S) (19.2%) and HDS + (N) (61.9%), than in the absence of this S-compound, HDN (10.6%). Similarly, the selectivity toward denitrogenated products (PCH and PB) was much higher in the HDS + (N) reaction than in the S-free HDN and HDN + (S) reactions (Table 5). Possible explanations of this behaviour include: (i), promotion of ring opening through a nucleophilic attack by hydrogen sulfide [45]; and (ii), as suggested by Nelson and Levy [46] C–N bond cleavage involves Hofmann degradation which is promoted by H^+ formed by H_2S dissociated on the catalyst surface.

3.3. Catalyst activity–structure correlation

It is well known that the formation of well-dispersed MoP species on the support surface is essential for the preparation of high-performance HDS catalysts. In this sense, surface properties such as acidity and specific area affect the dispersion and the local environment of the MoP species. This was confirmed in this study because both XRD and HRTEM data have demonstrated that the catalysts prepared by reduction of dried precursor (without calcination) shows a better distribution of the active phase than their counterpart prepared by reduction of calcined precursor at 700 °C. It was found a clear correlation between the total acidity and specific surface area and the catalysts activity, expressed as HDS reaction rate per surface exposure of MoP phase for the catalysts prepared by both methods (Fig. 9). As can be seen in Fig. 9, the MoP-c/r700 catalyst shows lower specific reaction rate than both catalysts prepared by the new method because the calcination process followed by reduction at higher temperature led to substantial decrease of acidity and S_{BET} due to the formation of MoP particles with a higher particle size. This correlation between particle size and catalytic activity in HDS over MoP based catalysts was also observed by Montesinos-Castellanos et al. [12]. These authors reported that the lower the particle size, the higher the amount of edge and kink sites on which DBT transformation takes place.

The catalytic activity showed by MoP-d/r550 catalyst underlines the viability of this preparation method to synthesize active MoP catalysts. Considering the type of phosphide precursors employed, the results are contrary to those reported recently by Gong et al. [24] indicating that the use of $NH_4H_2PO_4$ as P source for the preparation of bulk MoP was most effective than the use of H_3PO_4 and $(NH_4)_3PO_4$. This strongly suggests that the effect of P precursor is

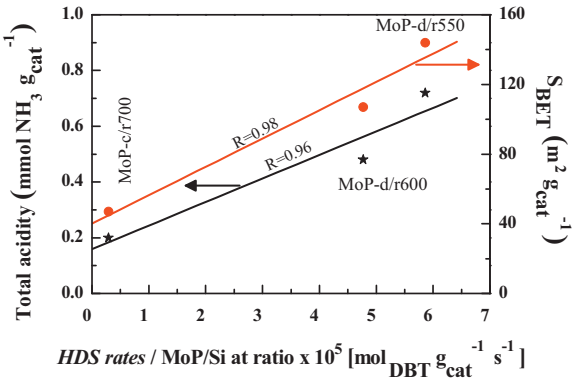

Fig. 9. Influence of total acidity (from TPD-NH_3) and specific surface area (from Table 1) on the specific reaction rates of the MoP catalysts prepared by different methods.

different for supported catalysts and another fact to consider is the lower reduction temperature needed for the reduction of dried precursor. The lower activity of the catalyst prepared from calcined substrate with respect to those prepared from dried precursors suggests that both texture and morphology of the MoP particles in the former sample are altered by the high reduction temperature (700 °C). Interestingly, contrary to bulk MoP catalysts [24], the catalysts prepared from H_2PO_3H phosphide precursor were stable during on-stream reaction, as confirmed by XPS.

The results obtained from CNHS elemental analysis for spent catalysts (Table 6) reveal the presence of great quantities of sulfur on the spent catalysts, while the amount of nitrogen is in all cases minimal. It could be thought that the absorption of DBT molecules on the catalysts surface is the responsible for such values. Nonetheless the proportion sulfur–carbon is hardly the same and that is why the presence of sulfur should be due not only to adsorbed DBT molecules but also to the formation of a MoS_2-type active phase. The formation of such a phase is observed in the XPS spectra of spent catalysts (Fig. 6), where a new Mo $3d_{5/2}$ band appears at ca. 229.0 eV (Table 3) and assigned in the literature to MoS_2 species [47] or to the incorporation of sulfur into the MoP structure during the catalytic test. Moreover MoP-c/r700 catalyst presents a S 2p band at ca. 161.0 eV (data not shown here) arising from the presence of S^{2-} ions. The formation of MoS_2 on this catalyst could be due to the presence of Mo^0 atoms present on the catalyst surface, and detected by XRD and XPS, that react with H_2S [48]. Notwithstanding, there is no evidence of the presence of metallic molybdenum on MoP-d/r550 catalyst, so the Mo $3d_{5/2}$ band at ca. 229.0 eV band should be also due to the incorporation of sulfur into MoP structure possibly forming a phosphosulfide phase, that has been considered the real active phase in transition metal phosphides. In this sense, the reaction where MoP-d/r550 catalyst presents better HDS and HDN results is that containing high DBT concentration (3000 ppm DBT + 200 ppm Q), and the amount of sulfur present in the spent catalyst is higher This strongly suggests that the enhancement of the HDS and HDN activity of MoP-d/r550 catalyst is due to the simultaneous presence of both MoP and MoS_2 type-active species on the catalyst surface. A similar effect was observed by Zuzaniuk and Prins [48] who detected an enhancement of the HDN activity of MoP/SiO_2 catalyst after the incorporation of sulfur to the catalyst.

Table 6
C, N and S contents[a] of spent MoP/SiO_2 catalysts[b] tested in HDS and HDN reactions.

Spent catalysts	% C	% N	% S
Effect of temperature			
MoP-d/r550 HDS	1.44	–	1.27
MoP-d/r600 HDS	1.99	–	1.01
MoP-c/r700 HDS	1.38	–	2.05
MoP-d/r550			
HDN	1.17	0.10	–
HDN + (S)	1.62	0.38	0.06
HDS + (N)	1.80	0.07	1.41
Stability test at 425 °C			
MoP-d/r550 HDS	2.74	–	2.85
MoP-d/r600 HDS	1.90	–	1.32
MoP-d/r550			
HDS + (N)	2.47	0.11	2.10
HDN + (S)	2.49	0.19	1.44

[a] As determined by elemental CNHS analysis.
[b] Feeds composition were: HDS reaction: 3000 ppm of DBT; HDN reaction: 3000 ppm of Q; HDN reaction + (S): 3000 ppm of Q + 200 ppm of DBT; and HDS reaction + (N): 3000 ppm of DBT + 200 ppm of Q.

4. Conclusions

In this study, silica-supported MoP catalysts were prepared using different P and Mo sources (H_2PO_3H versus $(NH_4)H_2PO_4$ and $(NH_4)_2MoO_4$ versus $(NH_4)_6Mo_7O_{24}{\cdot}4H_2O$). The temperature for precursor transformation upon H_2-reduction into molybdenum phosphide catalysts strongly depends on P and Mo precursors employed; being this temperature decisive for the specific characteristics of the MoP/SiO_2 systems. The reduction temperature is lowered for dried precursor due to: (i) the presence of P precursor having a lower oxidation state; (ii) the usage of molybdate instead of heptamolybdate, which should also be easier to reduce; and (iii) the absence of calcination step. The softer reduction conditions needed for the formation of MoP phase going from dried to reduced sample preserves the catalyst specific area, acidity and formation of smaller MoP clusters on the catalyst surface (from HRTEM) and therefore provides silica-supported MoP catalysts more active in the HDS of DBT reaction. MoP/SiO_2 catalyst prepared from the new synthetic approach was also active in simultaneous HDS and HDN reactions. While the quinoline conversion is enhanced in the presence of a small amount of DBT, the HDS of DBT reaction does not appear to be inhibited by a small amount of quinoline added to the feed.

Acknowledgements

We gratefully acknowledge the support from the Ministry of Science and Innovation, Spain (Ministerio de Ciencia e Innovación, España) through the project MAT2009-10481 and FEDER funds. A.I.M. thanks the Ministry of Science and Innovation, Spain (MICINN) for a Juan de la Cierva contract.

References

[1] D.J. Sajkowski, S.T. Oyama, Appl. Catal. A: Gen. 134 (1996) 339–349.
[2] M. Lewandowski, A. Szymańska-Kolasa, P. Da Costa, C. Sayag, Catal. Today 119 (2007) 31–34.
[3] M. Nagai, Appl. Catal. A: Gen. 322 (2007) 178–190.
[4] S.T. Oyama, J. Catal. 216 (2003) 343–352.
[5] S.T. Oyama, T. Gott, H. Zhao, Y.K. Lee, Catal. Today 143 (2009) 94–107.
[6] A.E. Henkes, Y. Vasquez, R.E. Schaak, J. Am. Chem. Soc. 129 (2007) 1896–1897.
[7] S.T. Oyama, Transition metal carbides, nitrides, and phosphides, in: G. Ertl, H. Knözinger, J. Weitkamp (Eds.), Handbook of Catalysis, Springer-Verlag, Weinheim, 2008.
[8] C. Stinner, R. Prins, Th. Weber, J. Catal. 202 (2001) 187–194.
[9] W. Li, B. Dhandapani, S.T. Oyama, Chem. Lett. 27 (1998) 2007–2008.
[10] D.C. Phillips, S.J. Sawhill, R. Self, M.E. Bussell, J. Catal. 207 (2002) 266–273.
[11] A. Montesinos-Castellanos, T.A. Zepeda, B. Pawelec, J.L.G. Fierro, J.A. de los Reyes, Chem. Mater. 19 (2007) 5627–5636.
[12] A. Montesinos-Castellanos, T.A. Zepeda, B. Pawelec, E. Lima, J.L.G. Fierro, A. Olivas, J.A. de los Reyes, Appl. Catal. A: Gen. 334 (2008) 330–338.
[13] S.T. Oyama, X. Wang, Y-K. Lee y, J. Chun, J. Catal. 221 (2004) 263–273.
[14] S.L. Brock, S.C. Perera, K.L. Stamm, Chem. Eur. J. 10 (2004) 3364–3371.
[15] S.L. Brock, K. Senevirathne, J. Solid State Chem. 181 (2008) 1552–1559.
[16] H. Loboué, C. Guillot-Deudon, A.F. Popa, A. Lafond, B. Rebours, C. Pichon, T. Cseri, G. Berhault, Ch. Geantet, Catal. Today 130 (2008) 63–68.
[17] L. Song, W. Li, G. Wang, M. Zhang, K. Tao, Catal. Today 125 (2007) 137–142.

[18] R. Cheng, Y. Shu, L. Li, M. Zheng, X. Wang, A. Wang, T. Zhang, Appl. Catal. A: Gen. 316 (2007) 160–168.
[19] S. Liu, Y. Qian, X. Ma, Mater. Lett. 62 (2008) 11–14.
[20] S. Burns, J.S.J. Hargreaves, S.M. Hunter, Catal. Commun. 8 (2007) 931–935.
[21] J.A. Cecilia, A. Infantes-Molina, E. Rodríguez-Castellón, A. Jiménez-López, J. Catal. 263 (2009) 4–15.
[22] J.A. Cecilia, A. Infantes-Molina, E. Rodríguez-Castellón, A. Jiménez-López, J. Phys. Chem. C 113 (2009) 17032–17044.
[23] J.A. Cecilia, A. Infantes-Molina, E. Rodríguez-Castellón, A. Jiménez-López, Appl. Catal. B: Environ. 92 (2009) 100–113.
[24] S. Gong, L. Liu, H. He, Energy Sources, Part A: Recovery, Utilization Environ. Eff. 33 (7) (2011) 641–648.
[25] S. Brunauer, P.H. Emmett, E. Teller, J. Am. Chem. Soc. 60 (1938) 309–319.
[26] S. Yang, C. Liang, R. Prins, Stud. Surf. Sci. Catal. 162 (2006) 465–469.
[27] Y. Shu, S.T. Oyama, Carbon 43 (2005) 1517–1532.
[28] P.A. Clark, S.T. Oyama, J. Catal. 218 (2003) 78–87.
[29] Y. Teng, A. Wang, X. Li, J. Xie, Y. Wang, Y. Hu, J. Catal. 266 (2009) 369–379.
[30] A. Montesinos-Castellanos, T.A. Zepeda, B. Pawelec, E. Lima, J.L.G. Fierro, A. Olivas, J.A.H. de los Reyes, Appl. Catal. A: Gen. 334 (2008) 330–338.
[31] Z.W. Yao, L. Wang, H. Dong, J. Alloys Compd. 473 (2009) L10–L12.
[32] Z. Wu, F. Sun, W. Wu, Z. Feng, C. Liang, Z. Wei y, C. Li, J. Catal. 222 (2004) 41–52.
[33] F. Rodriguez-Reinoso, J. Roquerol, K.S.W. Sing, K.K. Unger (Eds.), Characterization of Porous Solids II, Elsevier, Amsterdam, 1991.
[34] G. Leofanti, M. Padovan, G. Tozzola, B. Venturelli, Catal. Today 41 (1998) 207–219.
[35] P. Liu, J.A. Rodriguez, T. asakura, K. Nakamura, J. Phys. Chem. B 109 (2005) 4575–4583.
[36] D. Briggs, M.P. Seah (Eds.), Practical Surface Analysis. Auger and X-Ray Photoelectron Spectroscopy, Wiley, New York, 1990.
[37] T.L. Barr, J. Phys. Chem. 82 (1978) 1801–1810.
[38] A. Infantes-Molina, J.A. Cecilia, B. Pawelec, J.L.G. Fierro, E. Rodríguez-Castellón, A. Jiménez-López, Appl. Catal. A: Gen. 390 (2010) 253–263.
[39] C.N. Satterfield, M. Modell, J.F. Mayer, AIChE J. 21 (1975) 1100–1107.
[40] M. Egorova, R. Prins, J. Catal. 221 (2004) 11–19.
[41] S.T. Oyama, X. Wang, K.Y.-K. Lee Bando, F.G. Requejo, J. Catal. 210 (2002) 207–217.
[42] T. Kawai, K.K. Bando, Y.-K. Lee, S.T. Oyama, W.-J. Chun, K. Asakura, J. Catal. 241 (2006) 20–24.
[43] M. Jian, R. Prins, J. Catal. 179 (1998) 18–27.
[44] M. Jian, R. Prins, Stud. Surf. Sci. Catal. 113 (1998) 111–123.
[45] R.M. Laine, Catal. Rev. Sci. Eng. 25 (1983) 459–474.
[46] N. Nelson, R.B. Levy, J. Catal. 58 (1979) 485–488.
[47] B. Pawelec, S. Damyanova, R. Mariscal, J.L.G. Fierro, I. Sobrados, J. Sanz, L. Petrov, J. Catal. 223 (2004) 86–97.
[48] V. Zuzaniuk, R. Prins, J. Catal. 219 (2003) 85–96.